PERGAMON

Scripta Materialia 45 (2001) 1117–1122

Scripta MATERIALIA

www.elsevier.com/locate/scriptamat

Macroscopic subdivision of columnar grain aluminium with $\{001\}\langle uv0\rangle$ orientations following low strain deformation

G.L. Wu[a], A. Godfrey[b*], W. Liu[a], and Q. Liu[ab]

[a]*Department of Materials Science and Engineering, Materials Research Centre, Tsinghua University, 100084 Beijing, China*

[b]*Materials Research Department, Risø National Laboratory, DK-4000 Roskilde, Denmark*

Received 9 May 2001; accepted 31 May 2001

Abstract

Macroscopic grain sub-division in columnar grain A1 with $\{001\}\langle uv0\rangle$ orientations was studied. Significant differences, both between columnar grains of similar orientation, and between the columnar grains and equivalent single crystals were observed. These differences can be attributed to either differing initial orientations and/or grain–grain interactions during deformation. © 2001 Acta Materialia Inc. Published by Elsevier Science Ltd. All rights reserved.

Keywords: Cold working; Aluminium; EBSP/EBSD

Introduction

The evolution of deformation microstructure at both the macroscopic [1–6] and microscopic [7–10] length scales shows a strong dependence, amongst other parameters, upon crystal orientation [1–6,9,11]. A detailed knowledge of the orientation dependence of microstructural evolution during deformation is therefore very important for the development of microstructural models of evolution. Nevertheless, as a consequence of the difficulty of tracking the same grain throughout deformation, few studies exist of the dependence of deformation behaviour on initial grain orientation in polycrystals. One way in which this problem can be addressed is by the investigation of columnar grain specimens [12,13], which is an ongoing project of our study. Such samples potentially also allow an investigation of grain–grain interactions, by comparing the evolution of grains with similar initial orientations, but with differing neighbouring

* Corresponding author.
E-mail address: awgodfrey@bigfoot.com (A. Godfrey).

PII: S1359-6462(01)01091-0

grains. As an initial study it is important to understand how the pattern of sub-division in the coarse columnar grains relates to that of single crystals of similar orientations, so that differences that may be attributable to either initial grain orientation differences, or grain–grain interactions, can be more readily identified.

Although the crystallography of deformation microstructures is most accurately determined in the transmission electron microscope (TEM), this technique is time consuming, and only allows the sampling of a small volume of the specimen. Electron backscatter pattern (EBSP) investigations enable the acquisition large amount of crystallographic data at high speed. The EBSP technique has therefore become a powerful complimentary tool for examining deformation microstructures, and is particularly suited for investigating macroscale grain sub-division behaviour.

Experimental

The material used was pure columnar grain aluminium prepared by directional solidification with average columnar grain diameter of ~500 μm. The initial orientations of the grains show a strong $\{001\}\langle uv0\rangle$ fibre texture, mainly centered on $\{001\}\langle 100\rangle$ (cube) and $\{001\}\langle 110\rangle$ (ND45° rotated cube), as shown in Fig. 1a. Unidirectional rolling deformation to 10% reduction was done using 300 mm diameter rolls operating at 18 r.p.m. at room temperature under homogeneous deformation conditions. During rolling, the columnar axis of the grains is parallel to ND (RD, TD and ND are the rolling, transverse and normal directions, respectively), as illustrated in Fig. 1b. After rolling, the deformation microstructure was investigated by EBSP on electropolished ND/RD sections using a LEO1530 thermal field emission gun scanning electron microscope. Automated scans were carried out using stage control with a 5 μm step size.

For each grain studied, the average orientation was determined by performing simple averaging, followed by renormalization, of the vector components of the orientations expressed as quaternions [14]. For each crystallite within the grain, the misorientation to the average orientation was calculated, using the angle:axis format, and taking the minimum angle solution in each case. The misorientation to the average was then decomposed into three successive rotations about TD, ND and RD, as described in Ref. [4]. Band spacing was measured perpendicular to the set of bands under consideration.

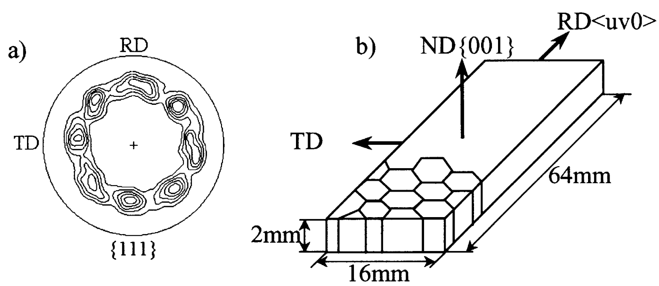

Fig. 1. (a) {1 1 1} pole figure of undeformed sample; (b) schematic diagram of the samples during rolling.

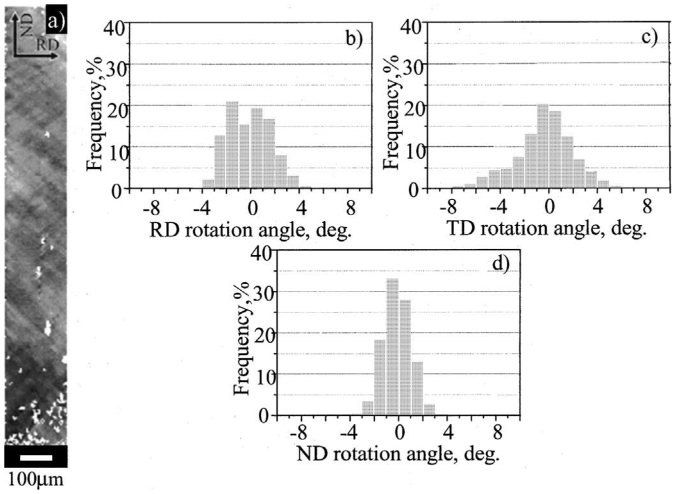

Fig. 2. Grain with near-cube orientation: (a) orientation image map constructed from TD component of partitioned rotation angles (white points correspond to non-indexed locations), and (b–d) histograms showing the distribution of RD, TD and ND partitioned rotation angle components, respectively.

Results

Fig. 2(a) shows an orientation image micrograph (OIM) of a grain with near-cube orientation (0.09 0.04 0.99) [0.97 −0.24 −0.08], misoriented from the ideal cube orientation by 14° about [0.17 −0.34 0.93]. The macroscopic sub-division of this grain is not immediately clear from this image, though two sets of fine scale bands, representing sub-division at a microscopic level, can be readily seen. These two sets of bands have a similar spacing of about 22 μm, and are aligned at about 40° to 45°, in opposite directions, to RD. The distributions of the partitioned RD, TD and ND components of the misorientation between each measurement point and the grain average are shown in Fig. 2(b–d). The TD angle component of the total rotation covers a wide range, from −7° to 6°, whilst the RD angle range is somewhat smaller, from −5° to 3°, and the ND rotation angle is only very small. The distribution of the rotation axes between each measurement point and the

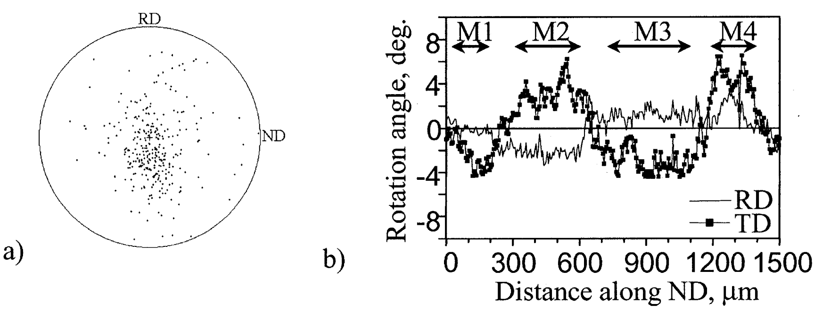

Fig. 3. Grain with near-cube orientation: (a) distribution of rotation axes between each measured orientation and the average before partitioning, (b) RD and TD partitioned rotation angle components for a scan along ND. The four matrix bands are marked M1 to M4. Each of these are separated by transition bands.

average grain orientation (Fig. 3a) confirms that the grain sub-division occurs mainly about TD, though with a significant RD component. Closer inspection of the TD and RD rotation angle components along a scan parallel to ND (Fig. 3b) reveals that this grain has sub-divided on a macroscopic scale, rotating mainly about TD by about 4–6°, in opposite directions, resulting in the formation of four matrix bands (regions of nearly uniform orientation [4,9]), connected by transition bands. Other near-cube orientation grains examined all showed grain sub-division predominately about the TD axis, though with a secondary rotation component either about the ND or RD direction. However, in some cube grains only two matrix bands, connected by one transition band, were observed.

Fig. 4(a) shows an OIM for a grain with orientation (−0.03 0.00 1.00)[0.80 0.61 0.03], misoriented from the ideal ND45° rotated cube by 8° around [0.21 0.03 0.98]. In this case, a macroscopic sub-division into two regions can be readily seen. In each of these two regions, one set of deformation bands with average spacing about 26 μm, lying at 30–40° to RD, is observed. Fig. 4(b–d) shows histograms for the distribution of the partitioned rotation angles about RD, TD and ND respectively. In contrast to the cube-oriented grains, the only significant grain rotation is about the TD direction (ranging from −11° to 9°), while the RD and ND rotation components are both mostly within 2°. This observation is confirmed by the tight clustering about TD of the rotation axes between each measurement point and the grain average (Fig. 5a). As the rotation angle components about RD and ND are small and non-systematic, Fig. 5b presents only the TD rotation angle component for a scan along ND. It is clear that the grain is macroscopically sub-divided by rotating predominately about TD in opposite directions by 6–10° to form two matrix bands connected by a narrow transition band. A similar pattern, both of grain-subdivision leading to two matrix bands rotated about TD in opposite directions, and micro-scale sub-division within these bands, was seen for grains of ND22° rotated cube orientation.

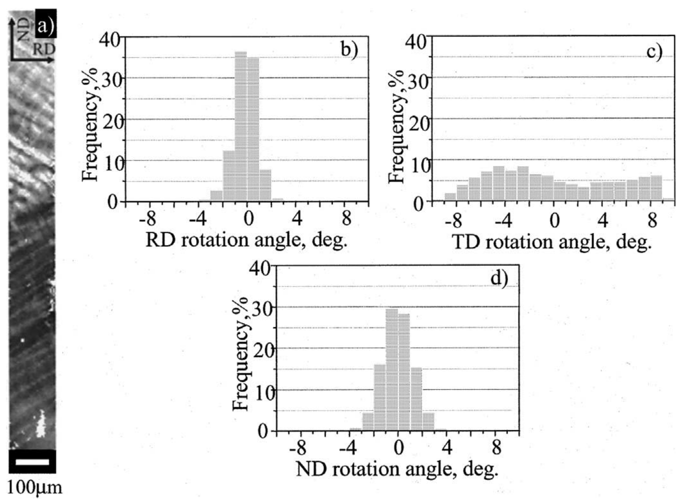

Fig. 4. Grain with near-ND45° rotated cube orientation: (a) orientation image map constructed from TD partition component of rotation angles (white points correspond to non-indexed locations), and (b–d) histograms showing the distribution of RD, TD and ND rotation angles, respectively.

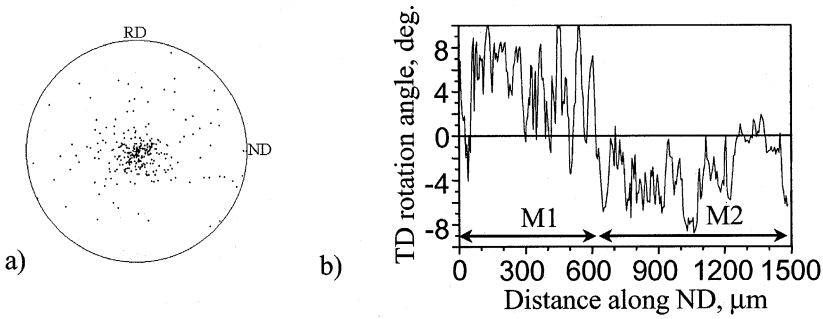

Fig. 5. Grain with near-ND45° rotated cube orientation: (a) distribution of rotation axes between each measured orientation and the average before partitioning, (b) RD and TD partitioned rotation angle components for a scan along ND. The two matrix bands are marked M1 and M2. The matrix bands are separated by a narrow transition band.

Discussion

In each of the columnar grains studied a macroscopic sub-division was found showing similar characteristics to the deformation pattern of single crystals of similar orientations, where the deformation microstructure following rolling deformation has been observed to comprise regions of similar orientation (matrix bands) separated by extended regions of cumulative orientation change (transition bands) [5,10]. In common with the single crystal equivalents, the predominant crystal rotation is about TD, with large cumulative TD rotations in the transition bands, leading to matrix bands rotated about TD in alternating senses. It is expected therefore that the kind of crystal plasticity analysis that has been applied to single crystals [10,15], should also be suitable for investigating the behaviour of the columnar grains. Despite the somewhat coarse EBSP step size used, and the low misorientation angles expected at this strain, the pattern of sub-division at the cell block level, as evidenced by the angles and spacing of bands within each matrix region, is also similar to that found by TEM investigations on single crystals of these orientations [10,16].

Several important differences can be noted however between the columnar grain and equivalent single crystal behaviour. For the cube-grains in single crystal rolling deformation, a pattern of four matrix bands is always observed, whereas for the columnar grains either two or four matrix bands were observed in near-cube oriented grains. Also the columnar grains of the cube-orientation show a grain sub-division pattern following rolling, more similar to the behaviour of the cube-orientation under channel die deformation, in which there is a significant RD rotation component in addition to the major TD rotation [2,17] (though for the columnar grains the strong secondary rotation was in some grains about ND). In contrast the only significant rotations in homogeneously rolled single crystals of these orientations are about TD [5,6]. The grains close to ND45° rotated cube and ND22° rotated cube orientations all exhibit just two matrix bands in the longitudinal plane, which is different to the results reported by Akef and Driver [2] of the single crystals in plane strain compression, in which a large number of matrix bands are found, in the longitudinal plane for the ND45° rotated cube orientation, and in both the longitudinal and compression plane for the ND22° rotated cube orientation.

It is known that the rotation path of the cube-oriented grains is sensitive to both the initial orientation and to variations of stress state [2–6,17]. It cannot be determined therefore from the current data set whether the differences between the columnar grains and their single crystal counterparts are attributable to variations of stress-state caused accommodations of stress and/or strain continuity at grain boundaries, or whether these differences are due to an differing initial grain orientation effect. Investigations tracking each initial grain orientation, and comparing the evolution of columnar grains with similar initial orientations, should be able to shed light on the extent of each of these effects. The existence of such differences in behaviour suggests however that the columnar grain samples are indeed suitable for such further investigations.

Conclusions

Macroscopic grain sub-division in columnar grain A1 with $\{001\}\langle uv0\rangle$ orientations, following cold-rolling to 10% reduction, leads to the development of matrix and transition bands associated predominantly by TD rotations, in general accord with the behaviour of single crystal samples of similar orientations. However significant differences, both between the columnar grains and equivalent single crystals, and between columnar grains of similar orientation, were also observed. Columnar grain samples are therefore expected to provide a useful means for studying the effect of differing initial orientations, and to investigate the transition between single and polycrystal grain deformation behaviour.

Acknowledgements

The authors wish to thank Drs. N. Hansen and D. Juul Jensen and for helpful comments and discussions. Financial support from the China National Youth Foundation, and from the Natural Sciences of Foundation of China under contract number 59825110, is gratefully acknowledged.

References

[1] Becker, R., Butler, J. F., Hu, H., & Lalli, L. A. (1990). Metall Trans A 22, 45.
[2] Akef, A., & Driver, J. H. (1991). Mater Sci Eng A 132, 245.
[3] Akef, A., & Driver, J. H. (1993). Texture Microstruct 20, 141.
[4] Wert, J. A., Liu, Q., & Hansen, N. (1997). Acta Mater 45, 2565.
[5] Liu, Q., & Hansen, N. (1998). Proc R Soc Lond A 454, 2555.
[6] Liu, Q., Maurice, C., Driver, J., & Hansen, N. (1998). Metall Mater Trans A 29, 2333.
[7] Bay, B., Hansen, N., Hughes, D. A., & Kuhlmann-Wilsdorf, D. (1992). Acta Metall Mater 40, 205.
[8] Kuhlmann-Wilsdorf, D., & Hansen, N. (1991). Scripta Metall 25, 1557.
[9] Liu, Q., Juul Jensen, D., & Hansen, N. (1997). Acta Mater 46, 5819.
[10] Hansen, N., & Juul Jensen, D. (1999). Phil Trans R Soc Lond A 357, 1447.
[11] Huang, X., & Hansen, N. (1997). Scripta Mater 37, 1.
[12] Hirsch, J., Nes, E., & Lücke, K. (1987). Acta Metall 35, 427.
[13] Tsuji, N., Takebayashi, N., Takiguchi, T., Tsuzaki, K., & Maki, T. (1995). Acta Metall Mater 43, 743.
[14] Krieger Lassen, N. C., Juul Jensen, D., & Conradsen, K. (1994). Acta Crystall A 50, 741.
[15] Liu, Q., Wert, J., & Hansen, N. (2000). Acta Mater 48, 4267.
[16] Wu, G. L., Godfrey, A., & Liu, Q., in preparation.
[17] Basson, F., & Driver, J. H. (1998). Mat Sci Forum 273–275, 313.